POAC'17
Busan, KOREA

Proceedings of the 24th International Conference on
Port and Ocean Engineering under Arctic Conditions
June 11-16, 2017, Busan, Korea

The Effects of Consolidation Time on the Strength and Failure Behavior of Freshwater Ice Rubble

Hamid Shayanfar[1, 2], Eleanor Bailey[1], Robert Pritchett[1], Rocky Taylor[1, 2]
[1] C-CORE's Centre for Arctic Resource Development, St. John's, Canada
[2]Memorial University of Newfoundland, St. John's, Canada

ABSTRACT

Ice ridges are common features in Arctic and sub-Arctic regions. They are large accumulations (typically 5-30 m) of ice rubble formed due to compressive or shear forces in ice cover. Understanding the deformation behavior and strength of ice rubble is key to estimating ice ridge loads on offshore structures. Medium-scale punch tests were conducted to measure and observe the strength and failure behavior of freshwater ice rubble. A custom-built punch box measuring 3.05 m in length and 0.94 m in width and height was used to perform the tests. The box walls were made from Plexiglas so that failure mechanisms could be observed. Ice rubble beams of nominal thickness 50 cm were produced by placing randomly sized ice pieces into the punch box, filled with water at its freezing temperature. After a specified consolidation time, the ice rubble beam was deformed by pushing a platen vertically downwards though the center of the beam until failure. Results showed that as the consolidation time varied from 0.2 to 70.5 hours, the failure behaviour changed considerably. For consolidation times less than 4 hours, the ice beam failed progressively and tended to fail by shearing; whereas, at times greater than 4 hours the beam failed by bending. The change in failure behaviour is controlled by the degree of bonding between ice blocks.

KEY WORDS: Ice rubble; Ridges; Consolidation time; Shear strength; Bending strength

NOMENCLATURE

η	Porosity
τ	Shear strength
σ	Bending strength
F_H	Hydraulic load
F_B	Buoyancy force
ρ_w	Density of water
g	Gravity
δ	Water level displacement
V_b	Nominal volume of submerged ice beam
A	Failure area
w	Box width
L	Box length

INTRODUCTION

Ice ridges are large accumulations of ice rubble that form due to compression or shear in the ice cover. They consist of two parts, a sail and a keel. The keel is the submerged part of an ice ridge, which is often frozen at the top forming what is often referred to as the consolidated or re-frozen layer. The non-submerged part of the ridge, the sail, is on average one fifth of the keel's depth (Timco et al, 2000). Ice ridges are complex features since they consist of individual ice blocks, random in size and orientation, and are bonded to each other with different degrees of strength from the consolidated layer to the base of the keel. Ridges are the thickest sea ice features in Arctic and sub-Arctic regions, and as such, must be considered during design loads estimation for vessels, offshore structures and subsea infrastructure.

A number of methods have been used to measure the mechanical properties of ice rubble. Initial tests began with the direct shear box test (Keinonen and Nyman (1978), Prodanovic (1979), Weiss et al., (1981), Hellmann (1984), Fransson and Sandkvist (1985)). Timco and Cornett (1999) reviewed these data and suggested that the wide range of data corresponded to the characteristics of the shear box setup, which induces non-uniform deformation and stress distribution in the ice rubble and forces the sample to fail along an induced failure plane (which may not be the weakest one). Other methods to investigate the mechanics of ice rubble included the shear box tests by Urroz and Ettema (1987), triaxial shear test by Gale et al. (1987) and Wong et al. (1990), biaxial shear tests by Timco et al. (1992), Sayed et al. (1992), Løset and Sayed (1993), Cornett and Timco (1995), and in situ punch tests conducted by Leppäranta and Hakala (1992), Croasdale and Associates Ltd. (1997, 1998) and Heinonen and Määttänen (2000).

Azarnejad and Brown (2001) and Lemee and Brown (2002) conducted laboratory scale punch tests on freshwater rubble to investigate the failure processes under more controlled conditions than are possible in the field. Azarnejad and Brown (2001) examined the influence that beam thickness (0.2 m-0.5 m), consolidation time (0-3 h) and hydraulic ram speed (9-120 mm s^{-1}) have on shear strength. They found that with higher consolidation time the cohesion and friction increased due to the development of freeze bonds between ice blocks. They also observed that at slow rates, ice beams behaved as a Mohr-Coulomb type material and the platen pushed a rectangular or trapezoidal plug out through the entire depth of the keel and failure occurred at the edges of the plug. At higher rates, failure occurred both under the platen as well as at a large surrounding area which had a triangular wedge. Lemee and Brown (2002) carried out similar tests using the same equipment but for larger ice rubble blocks and yielded comparable results. They also argued that ice rubble of larger dimensions fail in higher displacement. They observed that the lower the initial temperature of the ice blocks, the more bonded the rubble.

In this paper, initial results from a series of medium-scale punch tests are described. The focus of this work was to investigate the influence consolidation time had on the strength and failure behaviour of a 50 cm thick rubble beam. Tests consisted of deforming an ice rubble beam by pushing a platen vertically though its center until failure occurs (see Figure 1). In each case two tests were conducted; the first on the undeformed rubble beam and, the second, on the deformed beam to investigate frictional properties between the ice rubble blocks. The load applied to the platen was measured using a load cell and hydraulic ram displacement with a string pot. Video cameras were strategically positioned around the punch box to observe failure processes.

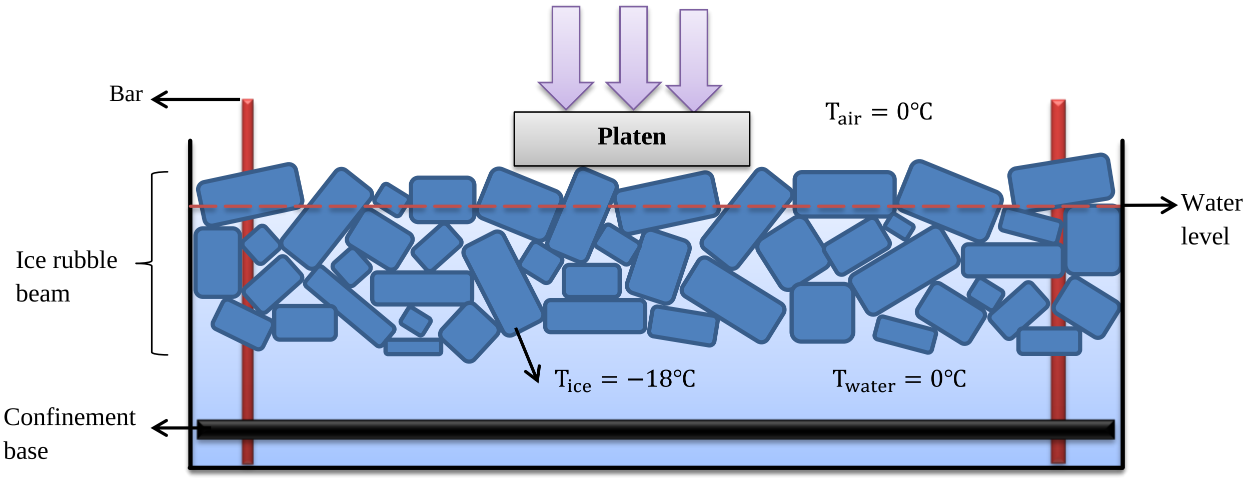

Figure 1. Schematic showing the punch test setup

APPARATUS AND INSTRUMENTATION

A custom-made punch box has been constructed for the test program that is 3.05 m in length and 0.94 m in width and height (see Figure 2). The walls are made from Plexiglas (with a grid drawn on) so that failure mechanisms and ice block motions can be observed and tracked. The punch platen is rectangular and spans the entire width of the box so that failure mechanisms can be observed. A platen width of 0.4 m was chosen based on careful consideration of how it will influence the failure of the beam and the block dimensions. Load was applied to the platen using a 20,000 lb (9 ton) hydraulic ram. To help make beams of even geometry, a bottom plate, mounted on 4 threaded rods, was brought up to produced beams that were 50 cm in thickness (see Figure 2).

During tests where the rubble was heavily bonded, the buoyancy of the non-loaded portion of the rubble was not sufficient to resist the applied load. As such, brackets had to be added to the end of the punch box to cause the beam to fail. This is similar to the procedure used by Azarnejad and Brown (2001) and Lemee and Brown (2002) where they glued small Plexiglas pieces on the tank walls to artificially increase friction between the tank walls and the ice rubble. The only difference being here that friction was only added to the ends of the box rather than the whole box to allow beams to fail in bending as well as shear.

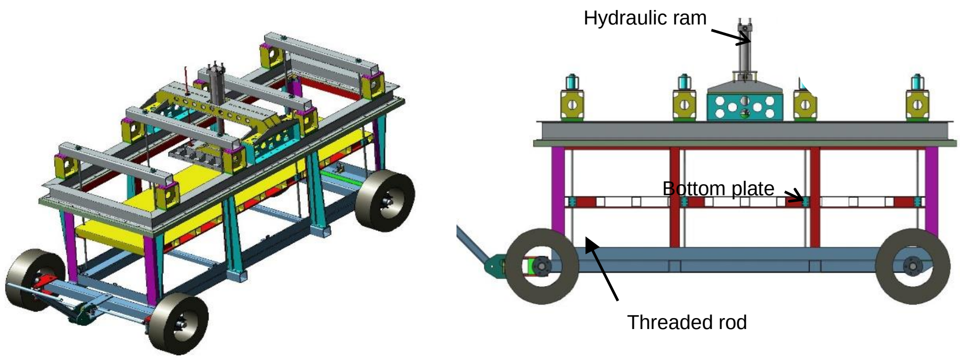

Figure 2. Computer aided design (CAD) images of the punch box assembly

A load cell was placed in line with the hydraulic ram to measure force applied to the rubble. A linear voltage displacement transducer (LVDT) was used to measure the vertical displacement and velocity throughout indentation. A total of six cameras were used to observe the punch box tests from different views. Four were placed side on to view the test through the Plexiglas window and two from the top (see Figure 3). A high speed video camera (HSV) was used to view the mid-point of the beam where the failure planes occurred, which is needed for calculating the shear strength. Three LED work lights were mounted on the opposite side of the punch box to illuminate the ice rubble beam. Cameras were synced with the load and displacement data through a noise trigger.

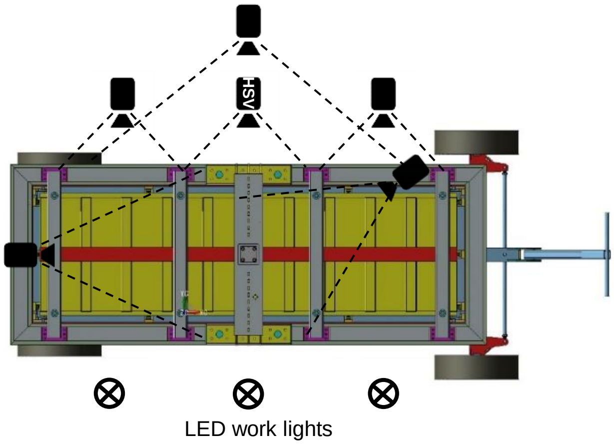

Figure 3. Camera and lighting locations

ICE RUBBLE PRODUCTION

Freshwater ice rubble was produced and stored in a refrigerated container. 1 m^2 pans were filled with tap water to an approximate depth of 10 cm and left to freeze at a nominal temperature of -18°C. Two dividers were placed in each pan prior to freezing to facilitate ice breakage. Once the water was frozen (approximately 5-6 days), pans were manually flipped over, allowing ice to break into randomly sized ice pieces. Larger sized ice pieces were broken with a hammer to give target lengths between 10 cm and 50 cm. Very small fragments and powdered ice which were less than 10 cm in thickness were swept away and thrown out. Figure 4 shows photographs of the reefer unit and the ice production methodology.

Figure 4. Ice rubble production and storage inside the refrigerated container

An analysis of the ice block dimensions was carried out to determine the ice block length, width and volume distributions. Photos of the ice blocks were taken during ice rubble fabrication and later analyzed using image processing software. Figure 5 shows that the length distribution of the ice blocks varied between 10 and 70 cm, with the majority falling in the range of 30 to 40 cm. The width distribution varied from 10 to 50 cm, with over 60% of the blocks being between the ranges of 20 to 30 cm. The length to width distribution shows that the ice blocks are generally square in shape with a maximum length to width ratio between 1 and 1.5.

Relatively large ice blocks were used in this test program so that the ice was ‘thermodynamically scaled’ to some extent. This we believe is particularly important to investigate the influence of consolidation time on the strength and failure behaviour of ice rubble as smaller ice blocks would not have sufficient cold reserves to form adequate freeze bonds. In addition, smaller ice pieces would result in a lower porosity and hence greater ice-ice contacts perhaps artificially increasing the rubble strength (Liferov and Bonnemaire, 2005).

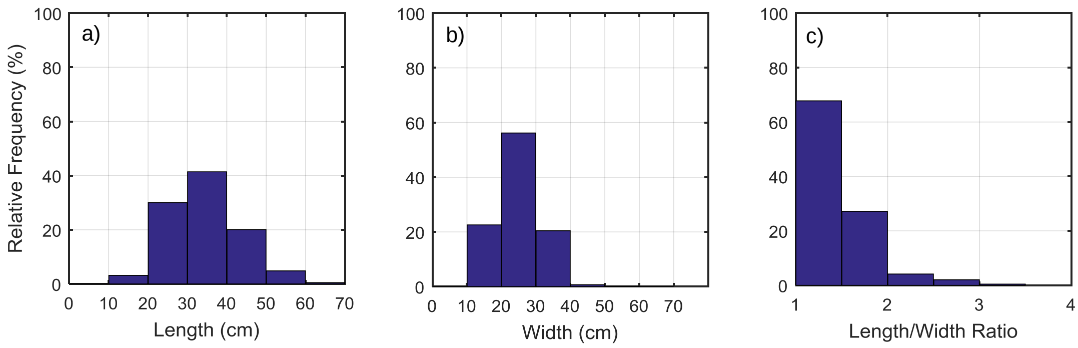

Figure 5. Histograms of the length (a), width (b) and length to width ratio (c) of the ice blocks

TEST PREPARATION & PLAN

The punch box tests were carried out in C-CORE’s cold room which was set to a nominal temperature of 0°C to keep the water as close to its freezing point as possible without a consolidated layer forming. Approximately 750 kg of ice rubble were needed to produce a 50 cm thick ice rubble beam. The mass of each ice rubble bag was measured using the crane scale, which is needed to derive porosity. Whilst loading the ice rubble into the punch box the bottom plate was positioned 50 cm from the top of the box, which helped to produce a beam of even geometry.

Once the ice rubble beam was prepared, the bottom plate was lowered and the box moved back into the cold room where the ice rubble blocks were left to consolidate for a set period of time. The ice rubble beam was then deformed at a constant rate of 5 mm s^{-1} until the beam failed. After each punch test, the hydraulic ram was retracted causing the rubble beam to settle back to its pre-test position. A second test was then performed that was referred to as the friction test as it was assumed that all bonds would have failed in the previous test and as such would be a measure of the friction and interlocking between ice rubble blocks.

A total of seven punch tests were carried out to investigate the influence consolidation time had on the strength and failure behaviour of an ice rubble beam (see Table 1). The consolidation time was varied from 0 to 70.5 hrs, whilst the initial ice temperature was held constant at -18°C. Note that while best efforts were made to conduct the test in “0 hrs” the fastest test setup time that has actually been achieved was 0.2 hrs (12 minutes).

Table 1. Test matrix

Test No.	Consolidation time (hrs)	Initial ice temperature (°C)	Block size
1	0.2	-18	(Length 30-40 cm; Width 20-30 cm)
2	2.4		
3	4.2		
4	4.4		
5	10.1		
6	28.5		
7	70.5		

RESULTS

Analysis of the video and load data from the test carried out after 0.2 hours of consolidation (see Figure 6) showed that a shear plug failure took place, where the central part of the beam was punched through while the non-loaded portion of the beam remained in place. Failure of the shear plug was progressive, where the first failure took place to the right of the platen at 52 mm of displacement, followed by a second failure to the left of the platen at 85 mm of displacement. The load trace from the friction test showed that no load drops were observed, demonstrating that as expected, the loads were associated with frictional and buoyancy forces with little or no bond failure. The higher loads observed in the punch test are likely due to a combination of interlocking between ice blocks or potentially some initial freeze-bonds that may have formed in the time it took to setup and run the test. The increase in load observed with displacement in both the punch and friction tests is due to increasing buoyancy forces as the ice beam is submerged further below the water.

The failure behaviour observed in the test conducted after 70.5 hours of consolidation (see Figure 7), was noticeably different from that done at 0.2 hours, where the beam failed in bending as opposed to shear. The load trace measured during the punch test showed a single failure at 65 mm of displacement. The failure plane was located slightly to the left of the platen, as opposed to the center which would be the case if the beam was homogenous. This is not unexpected as the distribution of the ice blocks in the rubble beam is random resulting in a non-uniform stress distribution. The loads measured in 70.5 hour friction test were significantly lower than those measured in the punch test, especially during peak load. This is because the rubble beam was heavily bonded in the punch test which increased the strength of the beam, whereas in the friction test, the bonds along the failure plane had already been broken.

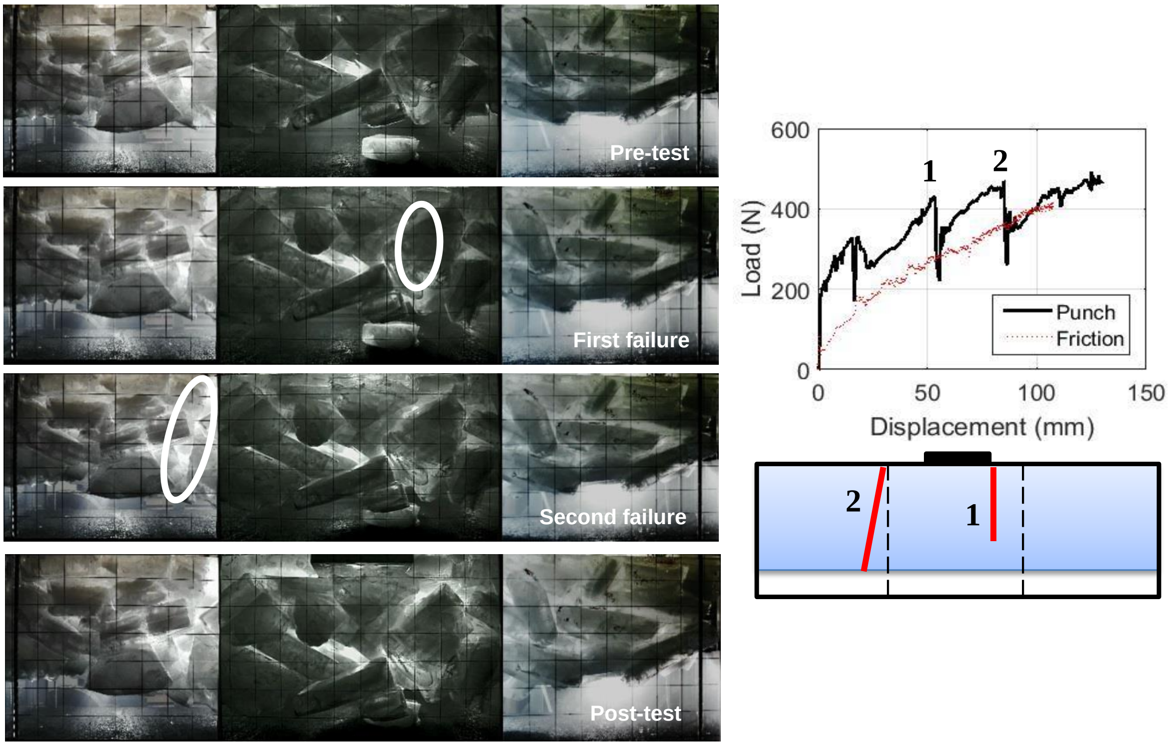

Figure 6. Analysis of video and load data from Test 1, which had a consolidation time of 0.2 hours, an initial ice temperature of -18°C, block size dimensions (length 30-40 cm, width 20-30cm) and an ice rubble beam thickness of 50 cm (see Table 1)

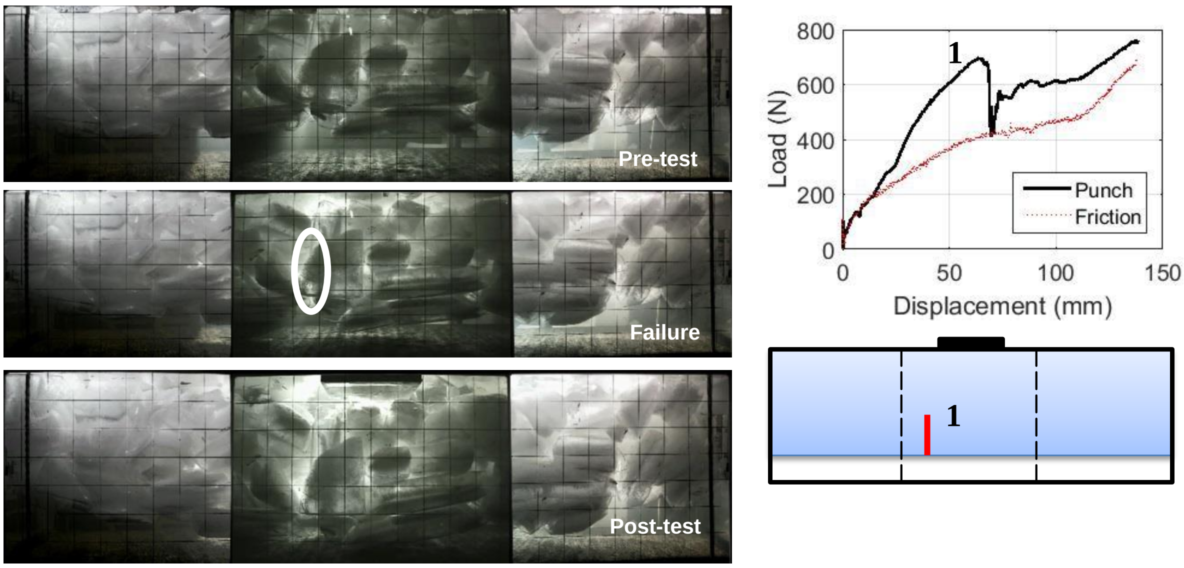

Figure 7. Analysis of video and load data from Test 7, which had a consolidation time of 70.5 hour, an initial ice temperature of -18°C, block size dimensions (length 30-40 cm, width 20-30cm) and an ice rubble beam thickness of 50 cm (see Table 1)

Figure 8 shows the force-displacement traces for all tests, as well as a schematic showing the observed failure behaviour of the beam. For consolidation times less than 4 hrs, the beam failed progressively in shear, where there were typically two load large drops observed before plug failure. For these shorter submersion times, since the bonds are expected to be weaker, a progressive sequence of block-block failures characteristic of macroscopic shear failure is more likely, which is analogous to shearing of a cohesive granular material. After 4 hrs of consolidation, the deformation behaviour appeared to change to a combination of bending and shearing or bending, where a single load drop resulted in failure of the beam. This behaviour may be attributed to increasing bonding which causes the rubble matrix to take on the behaviour of a brittle porous solid, in which higher stresses can be transmitted throughout the matrix resulting in macroscopic beam-like behaviour characterized by flexural failure. The peak load at failure increased with consolidation time from 460 N in the 0.2 hour test to 1400 N in the 4.4 hrs test, after which, it reduced to 700 N after 28.5 hrs of submersion. It is interesting that the 4.2 hrs test was much lower than the 4.4 hrs test (Tests 4 and 5 in Table 1), which was essentially a repeat test. This is possibly due to differences in setup times (where ice may have warmed up) or differences in the distribution of the blocks between the two tests. Additional repeat tests are needed to understand this discrepancy in more detail.

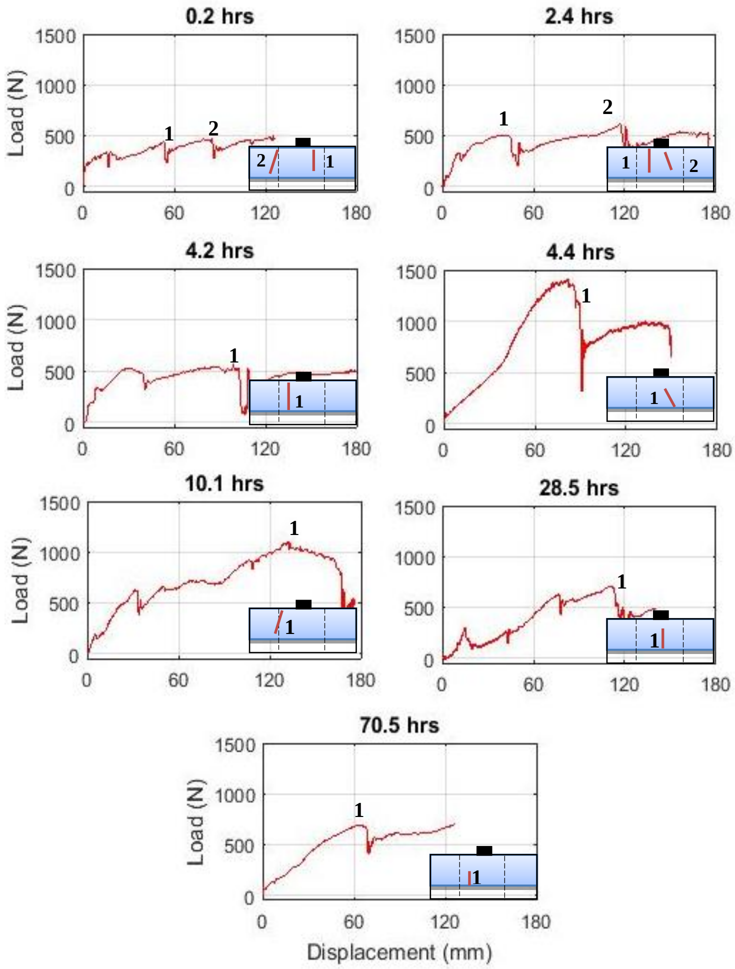

Figure 8. Force-displacement plots for all the punch box tests

DATA ANALYSIS

In order to measure the shear and bending strength of ice rubble, the buoyancy force must be calculated for each test. Two methods have been used to calculate the buoyancy force at the time of beam failure. In the first method, the rise in water level, δ, was used to estimate the buoyancy force at failure,

$$F_B = \delta w L \rho_w g \text{ [N]} \tag{1}$$

where ρ_w is the density of water, g is gravity and w and L are width and length of the box, respectively. δ was estimated from the height of the water level before the test (y_0) and at beam failure (y) i.e. $\delta = y - y_0$ (see *Figure 9*a). In the second method, the displacement observed at the underside side of the beam was used to estimate the buoyancy force at failure,

$$F_B = (1-\eta)\rho_w g V_b \text{ [N]} \tag{2}$$

where V_b is the nominal volume of the displaced ice beam. V_b was determined from the video data where the position of the underside of the beam pre and post failure are shown in solid and lines, respectively (see *Figure 9*b). It is the product of the displacement-length plot area (S in Figure 9) and the box width. Note that this method assumes that the displaced volume at the underside of the beam is equal to the submerged volume at the top of the beam (i.e. no compaction of expansion took place).

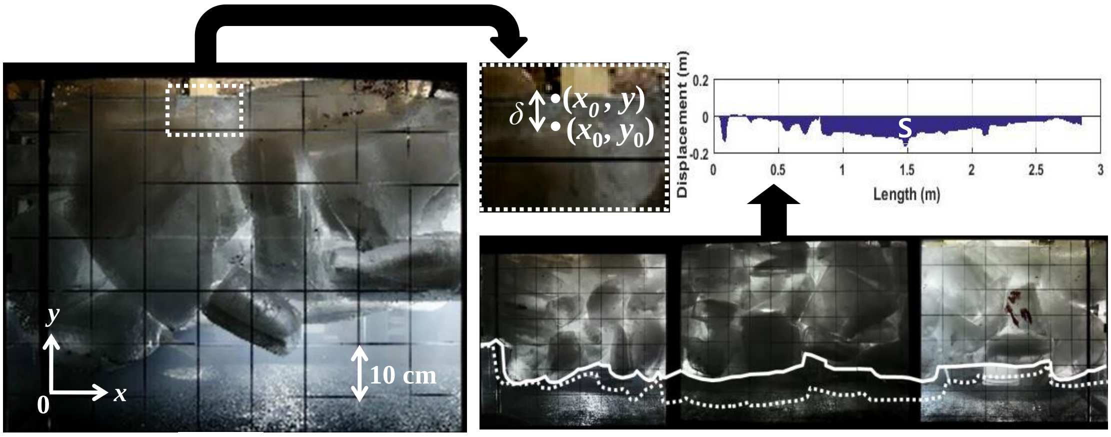

(a) (b)

Figure 9. Snap shots of the video data showing how the water level displacement (δ) and the displaced beam volume (V_b) were estimated for the buoyancy force calculations used in method I (a) and method II (b), respectively. Note that the grid on the box is 10 cm^2.

The estimated buoyancy force at failure was calculated for each test using both method I and II (Table 2). Results for both methodologies are presented here, not only for comparison, but also because in Test 3 one of the cameras malfunctioned so we were not able to observe the full beam and in Test 6 the water level was above the viewing panel. The buoyancy forces estimated using both methodologies were similar for all tests with the exception of Test 5. We are uncertain why the buoyancy force calculated using method II in Test 5 was higher than that calculated using method I. It was, however, noted that in this test the beam failed at a much greater ram displacement. This could have resulted in greater tensile splitting at the bottom of the beam resulting in an increased porosity (which was assumed to be constant in

Eq. 2). Table 2 shows that with increasing hydraulic ram displacement the buoyancy force increases.

The shear and bending strength of the ice rubble beam was estimated from the following equations,

$$\tau_{shear} = \frac{F_H - F_B}{A} \text{ [kPa]} \quad (3)$$

$$\sigma_{bending} = \frac{3(F_H - F_B)L}{2wh^2} \text{ [kPa]} \quad (4)$$

where *A* is the observed failure area, F_H is the peak load at failure and *L*, *w* and *h* are length, width and thickness of the ice beam, respectively. The buoyancy force used to calculate the shearing/bending strength was taken as the average of both methodologies when possible. In Table 3 the shear and bending strengths for different consolidation times are given. No values was given for Test 3, as previously mentioned, the HSV camera malfunction so the failure area could not be determined.

Table 2. Estimated buoyancy force at peak load

Test No.	Consolidation time (hrs)	Hydraulic ram displacement (mm)	Porosity	Buoyancy force (N)		Average buoyancy force (N)
				Method I	Method II	
1	0.2	84.84	0.39	396	346	371
2	2.4	116.9	0.38	561	600	580.5
3	4.2	100.5	0.37	528	-	528
4	4.4	80.61	0.34	682	661	671.5
5	10.1	132.1	0.44	695	920	807.5
6	28.5	106.5	0.42	-	448	448
7	70.5	64.25	0.41	504	489	496.5

Table 3. Estimated shear/bending strength at peak load

Test No.	Consolidation time (hrs)	Observed mode of failure	Shear strength (kPa)	Bending strength (kPa)
1	0.2	Shear	0.24	-
2	2.4	Shear	0.1	-
3	4.2	-	-	-
4	4.4	Bending	-	14.3
5	10.1	Bending	-	5.5
6	28.5	Bending	-	4.94
7	70.5	Bending	-	3.82

DISCUSSION AND CONCLUSION

A total of seven punch box tests were conducted to investigate the influence that consolidation time has on the strength and failure behaviour of a 50 cm thick freshwater ice rubble beam. Results showed that as the consolidation time varied from 0.2 hrs to 70.5 hrs, the failure behaviour changed considerably. For consolidation times less than 4 hrs, the ice beam failed progressively and tended to fail by shearing, whereas at times greater than 4 hrs the beam failed in a combination of shearing and bending or pure bending. The change in failure behaviour is controlled by the degree of bonding between ice blocks, where at low consolidation times the rubble was less bonded and behaved more like a cohesive granular material. At greater consolidation times the increased bonding caused the rubble to behave like a porous solid.

Due to the different failure modes observed, the data were analyzed both in terms of a shear and bending strength. At low consolidation times (0 to 2.4 hrs), the shear strength of the rubble varied from 0.1 kPa to 0.24 kPa with an average of 0.17 kPa. These are similar to the values report by Azarnejad and Brown (2001), which is surprising considering the different test setup, block size dimensions, initial ice temperatures and ram speeds. At higher consolidation times (4.4 to 70.5 hrs), the flexural strength varied from 3.82 kPa to 14.3 kPa with an average of 7.14 kPa.

Given the results presented here it is clear that the failure behaviour of the rubble changes considerably with consolidation time. In such cases it may not be correct to assume the rubble fails in pure shear, as is currently done in most ice ridge loading models, but rather a combination of shear and bending. Further work is currently ongoing to investigate these processes in more detail.

ACKNOWLEDGEMENTS

The authors would like to thank Ken Croasdale for many useful discussions and the Hibernia Management and Development Company, Ltd. (HMDC) and the Research and Development Corporation of Newfoundland and Labrador (RDC) for their financial support.

REFERENCES

Azarnejad, A., & Brown, T., 2001. Ice rubble behavior in punch test. *Journal of Cold Regions Engineering*, 15(3), pp. 135-153.

Cornett, A., & Timco, G., 1995. Laboratory tests on the mechanical properties of saline ice rubble . NRC Report HYD-CTR-002, 171 pp.

Croasdale & Associates, 1997. In situ Ridge Strength Measurements. A study sponsored by NRC (PERD) and Exxon Production Research Co.

Croasdale & Associates, 1998. In situ Ridge Strength Measurements. A study sponsored by NRC (PERD) and Exxon Production Research Co.

Fransson, L., & Sandkvist, J., 1985. Brash ice shear properties - laboratory tests. *Proceedings of the 8th International Conference on Port and Ocean Engineering under Arctic Conditions*, Narssarssuaq, Greenland, vol. 1, pp. 75-87.

Gale, A., Wong, T., Sego, D., & Morgenstern, N., 1987. Stress-strain behavior of cohesionless broken ice. *Proceedings of the 9th International Conference on Port and Ocean Engineering under Arctic Conditions*, Fairbanks, AK, vol. 3, pp. 109-119.

Heinonen, J., & Määttänen, M., 2000. LOLEIF ridge-loading experiments-analysis of rubble strength in ridge keel punch test . *Proceedings of the 15th International Symposium on Ice*, Gdnask, Poland, vol.1, pp. 63-72.

Hellmann, J., 1984. Basic investigations of Mush Ice. *Proceedings of the 7th International Symposium on Ice*, Hamburg, Germany, vol.3, pp. 37-55.

Keinonen, A., & Nyman, T., 1978. An experimental model-scale study on compressible,frictional and cohesive behavior of broken ice masses. *Proceedings of the International Symposium on Ice*, Lulea, Sweden. Vol. 2, pp. 335-353.

Lemee, E., & Brown, T., 2002. Small-scale plane strain punch tests. *Proceedings of the 16th IAHR International Symposium on Ice*, Dunedin, New Zealand, vol. 2, pp. 1-8.

Leppäranta, M., & Hakala, R., 1992. The structure and strength of first-year ridges in the Baltic Sea. *Cold Regions Science and Technology* 20, pp. 295-311.

Liferov, P., & Bonnemaire, B., 2005. Ice rubble behaviour and strength: Part I. Review of testing and interpretation of results. Cold Regions Science and Technology 41, pp. 135-151.

Løset, S., & Sayed, M., 1993. Proportional strain tests of fresh water ice rubble. *Cold Regions Science and Technology* 7 (2), pp. 44-61.

Prodanovic, A., 1979. Model tests of ice rubble strength. *Proceedings of the 5th International Conference on Port and Ocean Engineering under Arctic Conditions*, Trondheim, Norway, pp. 89-105.

Sayed, M., Timco, G., & Lun, L., 1992. Testing ice rubble under proportional strains. *Proceedings of Offshore Mechanics and Arctic Engineering Conference*, Calgary, Canada. pp. 335-341.

Timco, G., & Cornett, A., 1999. Is ρ a constant for broken ice rubble? *Proceeding of the 10th Workshop on River Ice Management with a Changing Climate*, Winnipeg, Manitoba, Canada. *pp. 318-331*.

Timco, G., Croasdale, K., & Wright, B., 2000. An Overview of First-Year Sea Ice Ridges. NRC Publications Archive, Canada.

Timco, G., Funke, E., Sayed, M., & Laurich, P., 1992. A laboratory apparatus to measure the behavior of ice rubble. *Proceedings of Offshore Mechanics and Arctic Engineering Conference*, Calgary, Canada, pp. 369-375.

Urroz, G. E., & Ettema, R., 1987. Simple-shear box experiments with floating ice rubble. *Cold Regions Science and Technology*, 14, 185-199.

Weiss, R., Prodanovic, A., & Wood, K., 1981. Determination of ice rubble shear properties . Proceeding of the International Symposium on Ice, Quebec, Canada, pp. 860-872.

Wong, T., Morgenstern, N., & Sego, D., 1990. A constitutive model for broken ice. *Cold Regions Science and Technology* 17, 241-252.